

Original paper

# The relationship between radiomic features in CT images and the salivary gland SPECT/CT standardised uptake value using 3D analysis

Yusaku Miki<sup>1,A,B,C,D,E,F</sup>, Ichiro Ogura<sup>2,E,F</sup>

<sup>1</sup>Department of Radiology, The Nippon Dental University Niigata Hospital, Niigata, Japan

<sup>2</sup>Department of Oral and Maxillofacial Radiology, The Nippon Dental University School of Life Dentistry at Niigata, Niigata, Japan

## ABSTRACT

**Purpose:** This study aimed to investigate the relationship between radiomic features extracted from computed tomography (CT) images and the mean standardised uptake value ( $SUV_{mean}$ ) obtained from salivary gland single-photon emission computed tomography (SPECT/CT), focusing on differences between Sjögren's syndrome and submandibular sialolithiasis.

**Material and methods:** Thirteen patients (7 with Sjögren's syndrome and 6 with submandibular sialolithiasis) underwent CT and SPECT/CT imaging.  $SUV_{mean}$  was calculated pre- and post-stimulation using technetium-99 m. Radiomic features were extracted from CT images using PyRadiomics, excluding shape-related features due to the impact of metal artifacts. Spearman's correlation coefficients were used to evaluate the relationship between pre/post-stimulation  $SUV_{mean}$  ratios and radiomic features. Regression models were created for features strongly correlated with  $SUV_{mean}$  ratios.

**Results:** The median pre/post  $SUV_{mean}$  ratios were 1.30 (1.02–1.57) for Sjögren's syndrome and 2.35 (2.23–3.01) for sialolithiasis. In Sjögren's syndrome, 4 radiomic features correlated strongly with the  $SUV_{mean}$  ratio: busyness ( $r = 0.78$ ,  $p < 0.01$ ), energy ( $r = 0.70$ ,  $p < 0.01$ ), total energy ( $r = 0.66$ ,  $p = 0.01$ ), and high grey level emphasis ( $r = -0.60$ ,  $p = 0.02$ ). No significant correlations were observed in sialolithiasis.

**Conclusions:** Specific radiomic features in CT images showed strong correlations with  $SUV$  ratios in Sjögren's syndrome but not in sialolithiasis. These findings suggest the potential utility of CT radiomics in evaluating salivary gland function, particularly in Sjögren's syndrome, providing insights into functional assessments without SPECT/CT.

**Key words:** Sjögren's syndrome, single photon emission computed tomography, radiomics.

## Introduction

Sjögren's syndrome is a chronic autoimmune disease characterised by dry eyes and mouth caused by dysfunction of the lacrimal and salivary glands [1]. This condition not only impairs salivary gland function but also significantly affects patients' quality of life due to chronic discomfort, inflammation, and oral health complications. Sialolithiasis is one of the most common salivary gland diseases pri-

marily affecting the submandibular gland, and the main clinical feature is pain and swelling associated with eating and subsequent sialadenitis [2]. While both conditions present distinct challenges, effective and accurate assessment of salivary gland function is essential for timely diagnosis and management.

Salivary gland scintigraphy has been widely used as an effective tool for assessing salivary gland excretion [3].

## Correspondence address:

Yusaku Miki, Central Radiology Department, Niigata Prefectural Cancer Center Hospital, Niigata, Japan, e-mail: [yusakumiki08@gmail.com](mailto:yusakumiki08@gmail.com)

## Authors' contribution:

A Study design · B Data collection · C Statistical analysis · D Data interpretation · E Manuscript preparation · F Literature search · G Funds collection

However, despite its usefulness for functional studies in Sjögren's syndrome and sialolithiasis, it remains a two-dimensional imaging modality. This limitation makes three-dimensional analysis and detailed quantitative evaluation of the salivary glands difficult. Furthermore, although computed tomography (CT) imaging provides detailed structural information, it is rarely used to diagnose Sjögren's syndrome. Using CT imaging alone to diagnose Sjögren's syndrome could provide a widely accessible and practical diagnostic option at many facilities.

Single-photon emission computed tomography (SPECT/CT), which combines three-dimensional imaging with functional data, has emerged as a powerful modality for assessing patients with head and neck lesions [4-6]. This technique enables detailed quantitative analysis, including the calculation of standardised uptake value (SUV), which is widely used for evaluating jaw lesions in bone SPECT/CT studies [7,8]. Recently, new software such as Xeleris 4DR and Q. Volumetrix MI has enhanced SUV analysis, offering improved operability and resolution [9,10]. The effectiveness of SPECT/CT in Sjögren's syndrome and submandibular sialolithiasis has been demonstrated [11,12].

Radiomics, a rapidly developing field in medical imaging, involves the extraction of a large number of quantitative features from medical images. By linking these features with biological information about lesions, radiomics can uncover subtle patterns that enhance diagnostic accuracy and improve treatment planning. Radiomics, or the science of extracting quantifiable data from standard-of-care radiologic images like CT images, could be considered the next generation of image evaluation, which has the potential to improve on the current standard [13]. In particular, radiomics has the potential to identify correlations between structural and functional imaging data, offering new insights into disease processes and their quantification.

Few studies, to our knowledge, have investigated the relationship between SUV obtained from SPECT/CT and radiomic features extracted from CT images in patients with salivary gland disorders. Moreover, comparing Sjögren's syndrome and sialolithiasis offers a unique opportunity to identify features specific to Sjögren's syndrome because these 2 conditions differ in both their underlying pathophysiology and patterns of gland dysfunction.

Therefore, this study aims to explore the relationship between SUV, a quantitative measure of parotid gland function, and CT-derived radiomic features in patients with Sjögren's syndrome and sialolithiasis. By comparing these 2 conditions, we seek to identify radiomic features that are specific to Sjögren's syndrome, providing new insights into its diagnosis and quantitative evaluation.

## Material and methods

### Patients

This study was approved by the ethical review board of Nippon Dental University Niigata Hospital (ESNG-R-280). Thirteen patients underwent CT imaging and SPECT/CT imaging at our hospital between December 2018 and January 2023. Seven patients were diagnosed with Sjögren's syndrome (0 men and 7 women; mean age: 56.1 years; range: 17-79 years), and 6 patients were diagnosed with submandibular sialolithiasis (4 men and 2 women; mean age: 51.3 years; range: 23-79 years). The diagnoses of Sjögren's syndrome were confirmed through the presence of autoantibodies and labial salivary gland biopsy [14,15]. The diagnoses of submandibular sialolithiasis were confirmed through surgical findings. Metal artefacts were observed in the CT images of 11 patients.

### SPECT/CT imaging and data analysis

SPECT/CT imaging was performed with a SPECT/CT scanner (Optima NM/CT 640; GE Healthcare, Tokyo, Japan) at 20 min (as pre-stimulation) and at 40 min (post-stimulation using 1.0 ml of citric acid) after injection of 370 MBq of technetium-99m pertechnetate (Technescinti; Nihon Medi-Physics, Tokyo, Japan), in accordance with our hospital protocol [11]. The  $SUV_{mean}$  of parotid glands was measured using a workstation and software (Xeleris 4DR and Q. Volumetrix MI; GE Healthcare, Tokyo, Japan), following our hospital protocol [9,10]. A volume of interest (VOI) on the SPECT/CT images was drawn over the parotid glands, and the  $SUV_{mean}$  within each VOI was analysed (Figure 1). For cases with metal artefacts, a VOI was created excluding those areas. The VOI was drawn by a radiation technologist, under the supervision of trained dental radiologists.

### CT images used to calculate radiomic features

CT imaging was performed with a 16-multidetector CT scanner (Aquilion TSX-101A; Canon Medical Systems, Otawara, Japan) using an oral and maxillofacial protocol at our hospital: tube voltage, 120 kV; tube current, 150 mAs; field of view, 240 × 240 mm; and rotation time, 0.50 s. The patients received non-contrast CT for head and neck lesions. In this study, we used 3D Slicer (<http://www.slicer.org/>) for parotid gland contour extraction and volume calculation. Contouring was performed slice by slice on transverse sections. Slices with metal artifacts were completely removed and contoured (Figure 2).

Radiomic features were calculated using Pyradiomics, an extension of the software 3D Slicer [16]. Segments were

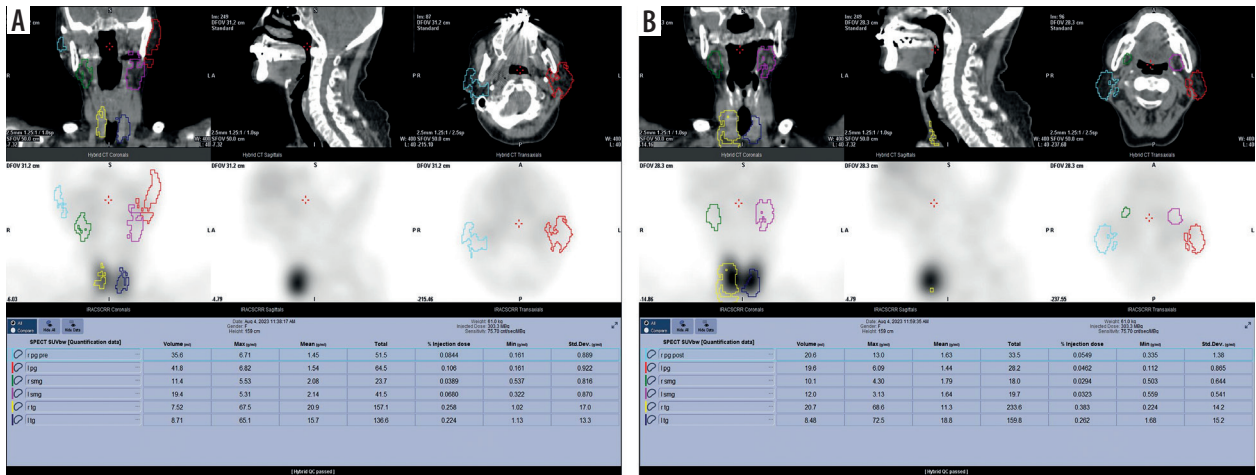


**Figure 1.** SPECT/CT in a 72-year-old woman with Sjögren's syndrome. The SUV<sub>mean</sub> of the right-parotid gland (red) and left-parotid gland (blue) for pre-stimulation were 1.45 and 1.54, poststimulation was 1.63 and 1.44, respectively (A and B)

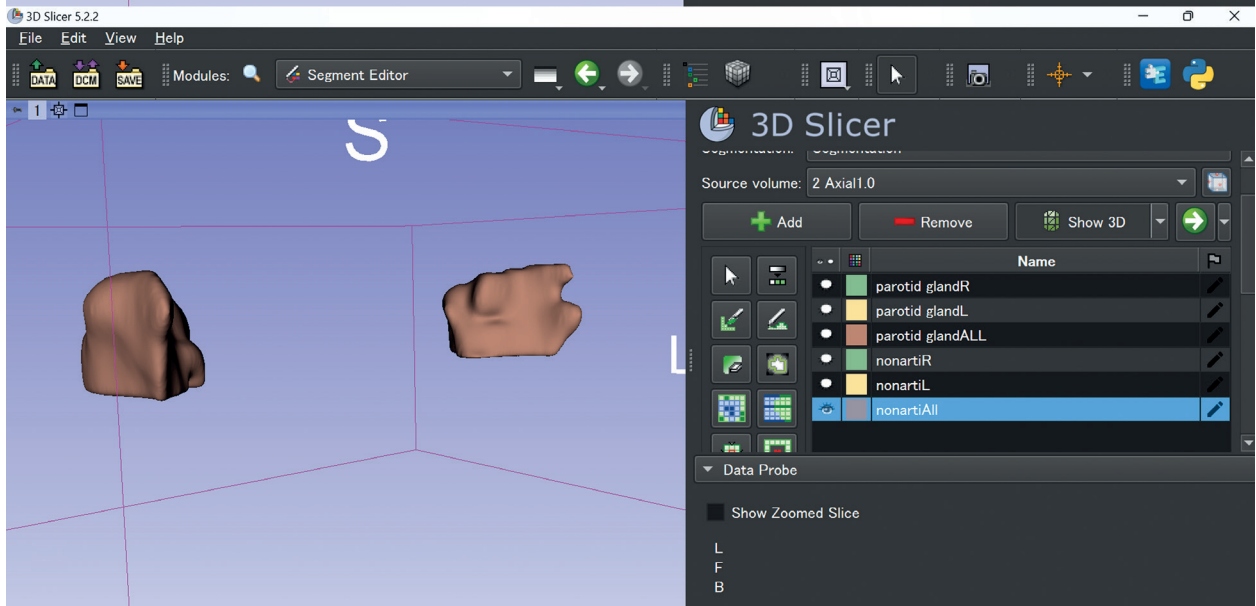
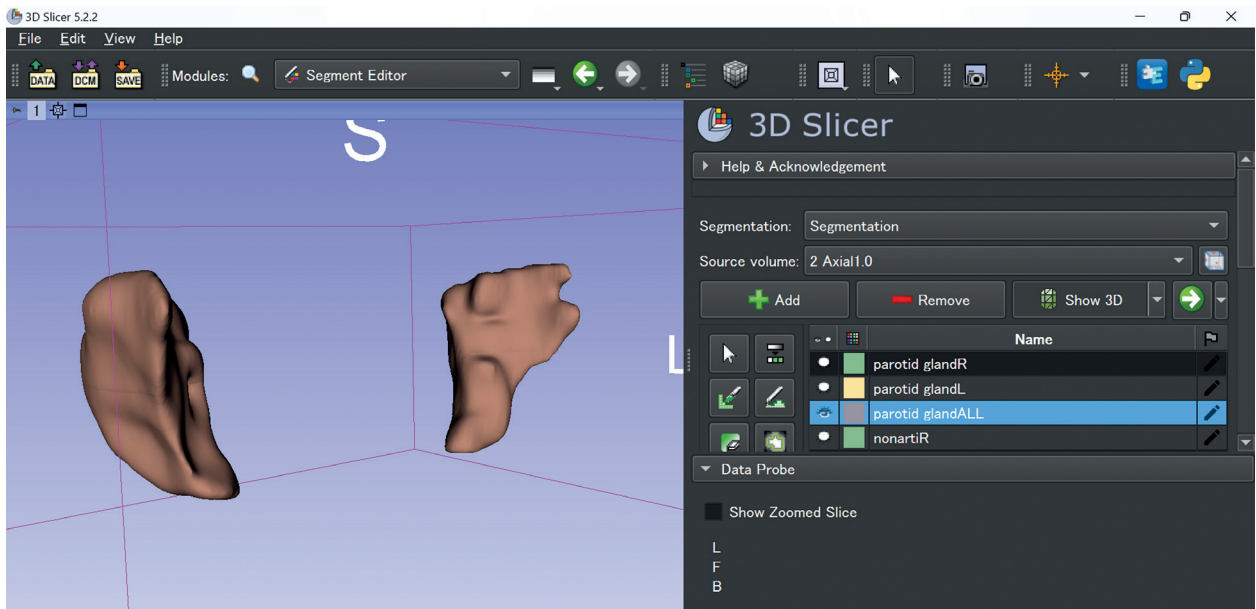


**Figure 2.** CT image of a 72-year-old woman with Sjögren's syndrome in 3D Slicer. Three-dimensional contour images created using 3D Slicer. (c) Image before contour deletion due to metal artefacts, (d) image after deletion

created in the CT images, and radiomic features were calculated. The bilateral parotid glands were calculated separately. A total of 107 radiomic features were extracted. However, 94 features were used for analysis because “Shape” features (14 in total) were excluded due to the potential impact of metal artefact removal on the calculation of radiomic features. The 94 radiomic features used in this study are listed in Table 1. The details of the features were referenced (<https://pyradiomics.readthedocs.io/en/latest/features.html#>).

### Statistical analysis

Spearman’s correlation coefficients were calculated to evaluate the relationships between  $SUV_{mean}$  and the 94 radiomic features, both pre- and post-stimulation. This method was chosen because the data did not follow a normal distribution.  $|r| = 0.6$  or more was considered to be strongly correlated. Statistical significance was defined

as a  $p$ -value  $< 0.05$ . For features that showed strong correlations with  $SUV_{mean}$ , simple regression equations were generated, and the adjusted  $R^2$  values were calculated to evaluate the explanatory power of the regression models. Statistical analysis was performed using EZR (Saitama Medical Centre, Jichi Medical University, Saitama, Japan; <https://www.jichi.ac.jp/saitama-sct/SaitamaHP.files/stat-medEN.html>).

### Results

The median (IQR) pre/post  $SUV_{mean}$  ratio for patients with Sjögren’s syndrome was 1.30 (1.02-1.57), while that for patients with sialolithiasis was 2.35 (2.23-3.01). In patients with Sjögren’s syndrome, correlations between pre/post  $SUV_{mean}$  ratio and radiomic features showed Spearman’s correlation coefficients greater than 0.6 for 4 features (Table 2). From highest to lowest: busyness in neighborhood gray tone difference matrix (NGTDM) ( $p < 0.01$ ,

**Table 1.** Types of 94 radiomic features obtained from 3D Slicer

Number and types of features	Feature name
18 types: First order	10Percentile, 90Percentile, Energy, Entropy, Interquartile, Range, Kurtosis, Maximum, Mean, AbsoluteDeviation, Mean, Median, Minimum, Range, RobustMeanAbsoluteDeviation, RootMeanSquared, Skewness, TotalEnergy, Uniformity, Variance
24 types: GLCM (gray level co-occurrence matrix)	Autocorrelation, ClusterProminence, ClusterShade, ClusterTendency, Contrast, Correlation, DifferenceAverage, DifferenceEntropy, DifferenceVariance, Id, Idm, Idmn, Idn, lmc1, lmc2, InverseVariance, JointAverage, JointEnergy, JointEntropy, MCC, MaximumProbability, SumAverage, SumEntropy, SumSquares
14 types: GLDM (gray level dependence matrix)	DependenceEntropy, DependenceNonUniformity, DependenceNonUniformityNormalized, DependenceVariance, GrayLevelNonUniformity, GrayLevelVariance, HighGrayLevelEmphasis, LargeDependenceEmphasis, LargeDependenceHighGrayLevelEmphasis, LargeDependenceLowGrayLevelEmphasis, LowGrayLevelEmphasis, SmallDependenceEmphasis, SmallDependenceHighGrayLevelEmphasis, SmallDependenceLowGrayLevelEmphasis
16 types: GLRLM (gray level run length matrix)	GrayLevelNonUniformity, GrayLevelNonUniformityNormalized, GrayLevelVariance, HighGrayLevelRunEmphasis, LongRunEmphasis, LongRunHighGrayLevelEmphasis, LongRunLowGrayLevelEmphasis, LowGrayLevelRunEmphasis, RunEntropy, RunLengthNonUniformity, RunLengthNonUniformityNormalized, RunPercentage, RunVariance, ShortRunEmphasis, ShortRunHighGrayLevelEmphasis, ShortRunLowGrayLevelEmphasis
16 types: GLSZM (gray level size zone matrix)	GrayLevelNonUniformity, GrayLevelNonUniformityNormalized, GrayLevelVariance, HighGrayLevelZoneEmphasis, LargeAreaEmphasis, LargeAreaHighGrayLevelEmphasis, LargeAreaLowGrayLevelEmphasis, LowGrayLevelZoneEmphasis, SizeZoneNonUniformity, SizeZoneNonUniformityNormalized, SmallAreaEmphasis, SmallAreaHighGrayLevelEmphasis, SmallAreaLowGrayLevelEmphasis, ZoneEntropy, ZonePercentage, ZoneVariance
5 types: NGTDM (neighborhood gray tone difference matrix)	Busyness, Coarseness, Complexity, Contrast, Strength

**Table 2.** Radiomic features strongly correlated with  $SUV_{mean}$  ratios

Feature type	Simple regression equation (adjusted $R^2$ )	Sjögren’s syndrome: Spearman’s correlation coefficient, $p$ -value	Submandibular gland sialolithiasis: $p$ -value
Busyness	$y = 3.3 \times +0.8$ (0.41)	$r = 0.78, p = 0.008$	0.33
Energy	$y = 9.8 \times 10^{-10} \times +1.1$ (0.27)	$r = 0.70, p = 0.03$	0.62
Total energy	$y = 9.0 \times 10^{-9} \times +1.0$ (0.38)	$r = 0.66, p = 0.01$	0.30
High gray level emphasis	$y = -4.4 \times 10^{-5} \times +2.0$ (0.31)	$r = -0.60, p = 0.02$	0.88

$SUV_{mean}$  – mean standardised uptake value

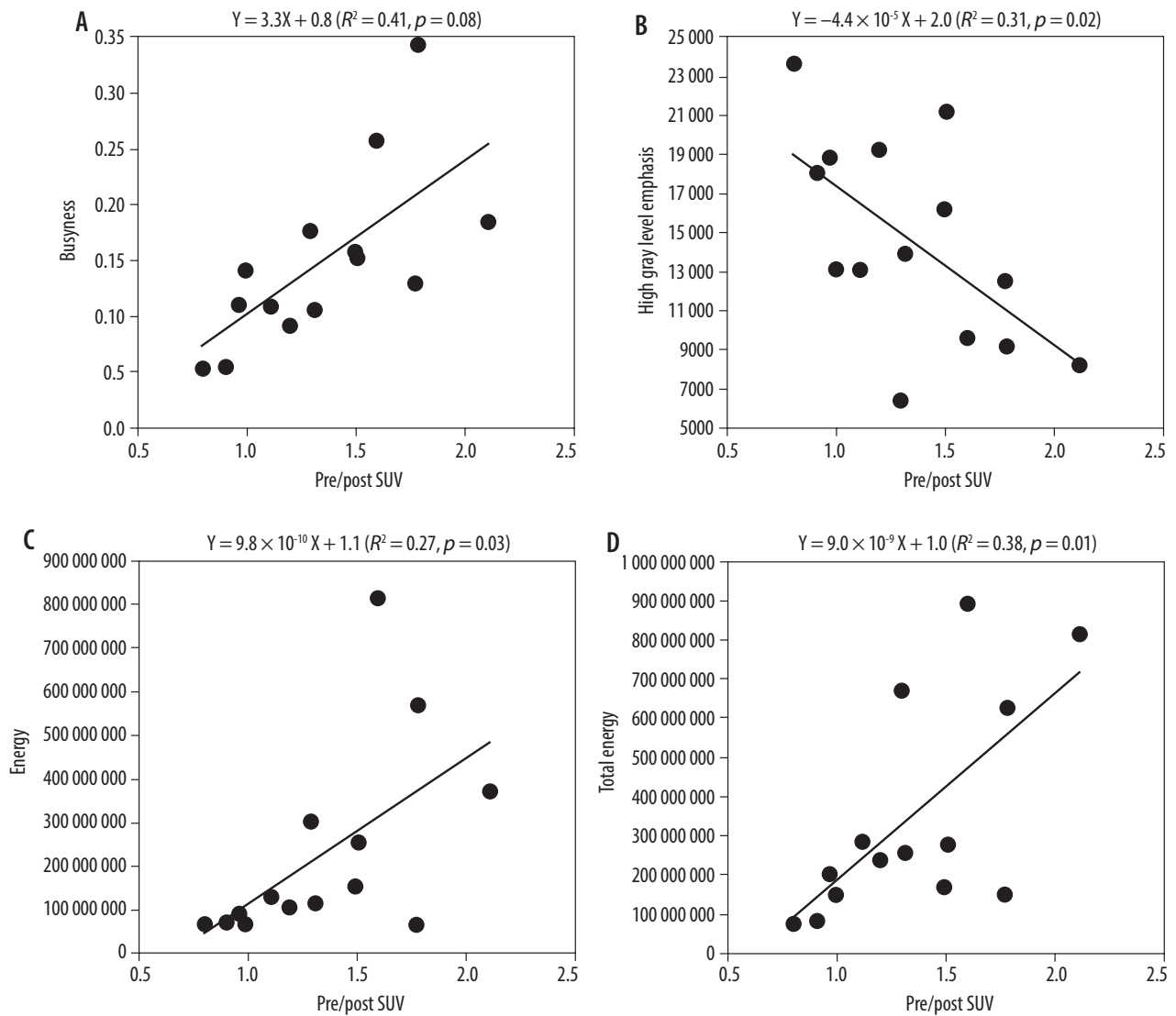


**Figure 3.** Correlations between pre/post SUV<sub>mean</sub> and 4 radiomic features in Sjögren's syndrome ( $n = 14$ )

$r = 0.78$ ), energy in first order ( $p < 0.01$ ,  $r = 0.70$ ), total energy in first order ( $p = 0.01$ ,  $r = 0.66$ ), high grey level emphasis in gray level dependence matrix (GLDM) ( $p = 0.02$ ,  $r = -0.60$ ) (Figure 3). In contrast, no radiomic features in patients with submandibular gland sialolithiasis showed strong correlations ( $|r| \geq 0.6$ ) with SUV<sub>mean</sub> ratios.

## Discussion

Research on the diagnosis of medical images using radiomic features has been active in recent years. The radiomics approach can automatically extract comprehensive data present in imaging modalities and uncover much more quantitative tumour information than our eyes can detect [17]. In a previous study, analysis of parotid tumours and parotitis was performed using radiomic features from CT images [18,19]. Although it is possible to determine Sjögren's syndrome using only CT images with high accuracy using deep learning, there are few studies on the relationship with salivary gland

function, such as SUV obtained with SPECT/CT [20]. The correlations with SUV<sub>mean</sub> obtained in this study provide information related to the severity of Sjögren's syndrome. This study is the first to directly compare SUV and radiomic features in SPECT/CT.

First, a high SUV<sub>mean</sub> before and after stimulation indicates normal parotid gland function with a large preSUV<sub>mean</sub> compared to postSUV<sub>mean</sub>. We will look at the value of each feature. Energy and total energy (first-order features): these features are calculated by squaring the CT values of each pixel and summing the results. Energy is used for local evaluation, whereas total energy is used for overall evaluation. Thus, higher values of these means higher image uniformity and higher pre/post SUV<sub>mean</sub> ratio. High grey level emphasis (GLDM): this feature highlights the concentration of high-intensity areas in CT images. A high value indicates localised high-intensity regions, suggesting fatty degeneration and fibrosis in the tissue, leading to a low pre/post SUV<sub>mean</sub> ratio. Busyness (NGTDM): This measures the density differences between

adjacent pixels. Higher values indicate smoother textures, signifying uniform tissue in CT images. Uniform parotid tissue suggests normal parotid gland function.

A comparison of parotid glands using magnetic resonance sialography and salivary gland scintigraphy revealed that pre/post  $SUV_{mean}$  ratios were higher in images with heterogeneous tissue, which aligns with the findings of this study [21]. Similar results were observed for  $SUV_{mean}$  [22]. Conversely, no radiomic features were identified as indicators of salivary lithiasis. This suggests that the 4 of the radiomic features analysed in this study are specific to Sjögren's syndrome. Furthermore, the findings indicate that CT imaging alone may provide functional information for patients with Sjögren's syndrome.

In contrast to previous studies that used the maximum standardised uptake value ( $SUV_{max}$ ), this study utilised  $SUV_{mean}$ , which is less dependent on the individual measurement of the ROI and offers higher reproducibility [11,22].

A key advantage of using 3D Slicer is that it is open-source software, accessible to any facility. Additionally, while many previous studies relied on two-dimensional ROI settings, this study employed three-dimensional ROIs, enabling a more comprehensive evaluation of the entire parotid gland.

This study is limited by its small sample size, necessitating validation with larger cohorts. As machine learn-

ing-based automatic diagnosis using radiomic features becomes increasingly common, future studies should aim to develop in this direction. Furthermore, excluding regions affected by metal artifacts limited the evaluation of those areas. Future studies should include patients without metal artifacts for more comprehensive analysis.

## Conclusions

There was a strong correlation between the  $SUV_{mean}$  ratio on SPECT/CT and radiomic features extracted from CT images in patients with Sjögren's syndrome. These findings suggest the potential utility of CT radiomics in evaluating salivary gland function, particularly in Sjögren's syndrome, providing insights into functional assessments without SPECT/CT

## Disclosures

1. Institutional review board statement: This study was approved by the ethical review board of Nippon Dental University Niigata Hospital. Approval number: ESNG-R-280.
2. Assistance with the article: None.
3. Financial support and sponsorship: None.
4. Conflicts of interest: None.

## References

1. Negrini S, Emmi G, Greco M, Borro M, Sardanelli F, Murdaca G, et al. Sjögren's syndrome: a systemic autoimmune disease. *Clin Exp Med* 2022; 22: 9-25.
2. Lafont J, Graillon N, Hadj Saïd M, Tardivo D, Foletti JM, Chossegros C. Extracorporeal lithotripsy of salivary gland stone: a 55 patient's study. *J Stomatol Oral Maxillofac Surg* 2018; 119: 375-378.
3. Ogura I, Hayama K, Sue M, Oda T, Sasaki Y. Submandibular sialolithiasis with CT and scintigraphy: CT values and salivary gland excretion in the submandibular glands. *Imaging Sci Dent* 2017; 47: 227-231.
4. Ogura I, Kobayashi E, Nakahara K, Igarashi K, Haga-Tsujimura M, Toshima H. Quantitative SPECT/CT imaging for medication-related osteonecrosis of the jaw: a preliminary study using volume-based parameters, comparison with chronic osteomyelitis. *Ann Nucl Med* 2019; 33: 776-782.
5. Ogura I, Sasaki Y, Sue M, Oda T, Kameta A, Hayama K. Tc-99m hydroxymethylene diphosphonate SPECT/CT for the evaluation of osteonecrosis of the jaw: preliminary study on diagnostic ability of maximum standardised uptake value. *Clin Radiol* 2020; 75: 46-50.
6. Oohashi M, Toshima H, Hayama K, Ogura I. Gallium-67 SPECT-CT for the evaluation of head and neck: preliminary study on maximum standardized uptake value in lesions, and in the parotid and submandibular glands. *Pol J Radiol* 2020; 85: e224-e229. DOI: 10.5114/pjr.2020.95458.
7. Toshima H, Ogura I. Assessment of inflammatory jaw pathologies using bone SPECT/CT maximum standardized uptake value. *Dentomaxillofac Radiol* 2020; 49: 20200043. DOI: 10.1259/dmfr.20200043.
8. Minami Y, Ogura I. Bone single-photon emission computed tomography-CT peak standardized uptake value for chronic osteomyelitis, osteoradionecrosis and medication-related osteonecrosis of the jaw. *J Med Imaging Radiat Oncol* 2021; 65: 160-165.
9. Minami Y, Ogawa R, Ogura I. Volumetric analysis of mandibular lesions with SPECT/CT: a pilot clinical study of maximum standardized uptake value. *Pol J Radiol* 2022; 87: e311-e315. DOI: 10.5114/pjr.2022.117569.
10. Tezuka Y, Ogura I. Maximum and mean standardized uptake values of medication-related osteonecrosis of the jaw with bone SPECT/CT: comparison of mandibular pathologies, control and temporomandibular joints. *Dentomaxillofac Radiol* 2023; 52: 20230119. DOI: 10.1259/dmfr.20230119.
11. Ninomiya K, Toya S, Ogura I. Single-photon emission computed tomography/computed tomography for evaluation of salivary gland dysfunction: preliminary study on diagnostic ability of maximum standardized uptake value. *Oral Radiol* 2020; 36: 163-167.
12. Minami Y, Ogura I. A clinical pilot study of salivary gland secretion for xerostomia patients with Sjögren's syndrome using SPECT/CT. *Gerodontology* 2022; 39: 297-301.
13. Kummar S, Lu R. Using radiomics in cancer management. *JCO Precis Oncol* 2024; 8: e2400155. DOI: 10.1200/PO.24.00155.

14. Greenspan JS, Daniels TE, Talal N, Sylvester RA. The histopathology of Sjögren's syndrome in labial salivary gland biopsies. *Oral Surg Oral Med Oral Pathol* 1974; 37: 217-229.
15. Ono J, Toya S, Ogura I, Okada Y. Study of clinical factors, focus score, lymphocyte type and NF- $\kappa$ B pathway in Sjögren's syndrome. *Odontology* 2023; 111: 207-216.
16. van Griethuysen JJM, Fedorov A, Parmar C, Hosny A, Aucoin N, Narayan V, et al. Computational radiomics system to decode the radiographic phenotype. *Cancer Res* 2017; 77: e104-e107. DOI: 10.1158/0008-5472.CAN-17-0339.
17. Lu Y, Liu H, Liu Q, Wang S, Zhu Z, Qiu J, et al. CT-based radiomics with various classifiers for histological differentiation of parotid gland tumors. *Front Oncol* 2023; 13: 1118351. DOI: 10.3389/fonc.2023.1118351.
18. Zhang D, Li X, Lv L, Yu J, Yang C, Xiong H, et al. A preliminary study of CT texture analysis for characterizing epithelial tumors of the parotid gland. *Cancer Manag Res* 2020; 12: 2665-2674.
19. Ito K, Muraoka H, Hirahara N, Sawada E, Tokunaga S, Kaneda T, et al. Quantitative assessment of the parotid gland using computed tomography texture analysis to detect parotid sialadenitis. *Oral Surg Oral Med Oral Pathol Oral Radiol* 2022; 133: 574-581.
20. Kise Y, Ikeda H, Fujii T, Fukuda M, Arijii Y, Fujita H, et al. Preliminary study on the application of deep learning system to diagnosis of Sjögren's syndrome on CT images. *Dentomaxillofac Radiol* 2019; 48: 20190019. DOI: 10.1259/dmfr.20190019.
21. Ogura I, Sasaki Y, Oda T, Sue M, Hayama K. Magnetic Resonance Sialography and Salivary Gland Scintigraphy of Parotid Glands in Sjögren's Syndrome. *Chin J Dent Res* 2018; 21: 63-68.
22. Shirai A, Ogura I. Maximum standardized uptake value for parotid and submandibular glands in patients with Sjögren's syndrome and submandibular sialolithiasis using salivary gland SPECT/CT. *Odontology* 2025; 113: 857-863.